Design of Microrings with Complex Waveguide Cross-Sections to Reduce Non-linear Effects of Silicon

Design of Microrings with complex waveguide cross-sections to reduce non-linear effects of silicon.

Stefania Cucco[1[0009-0006-4627-0606]], Marco Novarese[1[0000-0001-8957-469X]] and Mariangela Gioannini[1[0000-0002-6250-5640]]

[1] Department of Electronic and Telecommunications, Politecnico di Torino.Torino, Italy
stefania.cucco@polito.it marco.novarese@polito.it
mariangela.gioannini@polito.it

Abstract. This study presents a model for designing silicon and polysilicon (poly-Si) micro-ring resonators (MRRs) within the semiconductor-insulator-semiconductor capacitor platform (SISCAP). It employs generic waveguide cross-sections, including complex rib structures, to address nonlinear effects and self-heating. We highlight the crucial role of free carrier diffusion in rib waveguides and Shockley-Read-Hall recombination in mitigating nonlinearities within the ring resonator. In particular, we introduce a novel method for 2D simulations of MRRs, incorporating self-consistent generation of free carriers via TPA, their transport, non-radiative recombination, heat generation, and dissipation. These factors alter the MRR transmission coefficient, significantly diminishing the quality factor (Q) as injected power increases. The amount of input power injected into the ring is limited when high Q values ($1.3 \cdot 10^5$) are considered. Our objective is to propose new designs capable of increasing the input power by an order of magnitude while limiting the Q degradation to less than 10%, which is crucial for enhancing MRR performance in various silicon photonics applications.

Keywords: Microring resonator, silicon, nonlinear effects.

1 Introduction

Microring resonators (MRRs) serve as passive optical components extensively utilized within silicon photonic integrated circuits, finding application across various photonics fields such as sensors, optical modulators, beam-steering, wavelength filtering, switching, and light modulation [1]. However, the nonlinear behavior of silicon, even under moderate input powers, presents challenges to achieving high Q-factor MRR performance. In this investigation, we present a rigorous simulation method to account for nonlinear and thermal effects in silicon MRRs featuring complex waveguide cross-sections. We apply this method specifically to optimize MRR designs within the SISCAP platform. This platform offers advantages in reducing both the cost and energy consumption of optical transceivers for optical interconnects, all while maintaining high data rates and volume across various applications [2].
Our study aims to improve the comprehension and performance of MRRs, which are crucial for advancing silicon photonics technologies.

2 Model

Silicon introduces notable nonlinear effects, in particular two-photon absorption (TPA) and free carrier absorption (FCA). TPA results from the absorption of two photons, generating an electron-hole pair, while FCA arises from free carriers absorbing additional photons, elevating electrons and holes to higher energy states in the conduction and valence bands. The presence of free carriers modifies the refractive index, causing a blue shift in the resonant wavelength of the MRR transmission coefficient, and contributes to FC loss, degrading the Q-factor. Additionally, thermalization and recombination via Shockley-Read-Hall (SRH) mechanisms release energy as heat (self-heating), inducing a red shift in the transmission coefficient. To simulate these nonlinear effects and self-heating in MRRs, we utilize 2D simulations incorporating FC generation through TPA, FC drift-diffusion transport, SRH recombination, and thermal dynamics. By evaluating the impact of nonlinear effects on MRRs for various input powers and generic waveguide cross-sections, as those shown in Fig.1(a), we improve our understanding of silicon photonics performance. Through a self-consistent model, integrating optical field distribution and solving drift-diffusion equations coupled with a thermal model, we obtain the distribution of free carriers and temperature variations, making it possible to compute the modal loss and refractive index changes due to free carriers and temperature fluctuations.

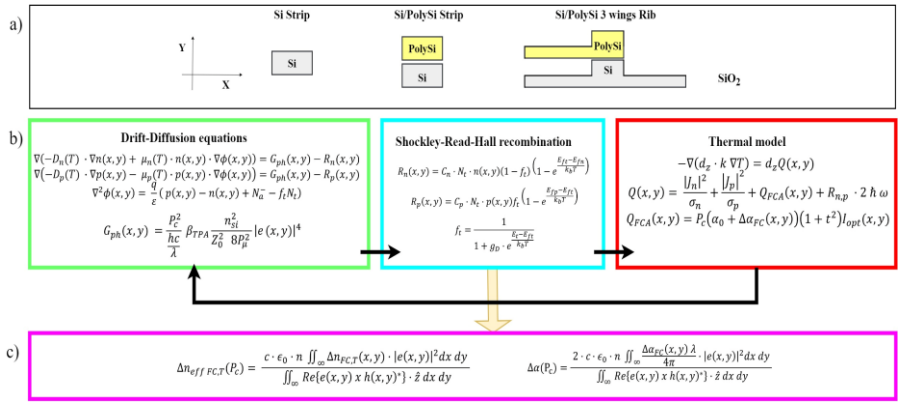

Fig. 1. (a) Cross sections of the waveguides. (b) Model summary. (c) Equations of effective refractive index variation and optical modal loss.

We summarize the self-consistent model, as shown in Fig.1 (b). we import in COMSOL Multiphysics (Semiconductor module with Thermal module) the spatial distribution of the fundamental guided mode optical field (e (x, y) and h (x, y)) in the ring waveguide and we solve self-consistently the drift-diffusion equations coupled with the thermal model. The solution provides the spatial distribution of free carriers, denoted as n(x, y) and p(x, y), and the temperature variation, represented as T(x, y), in relation to the circulating power across the waveguide cross-section. Having then the local variation of FC loss and refractive index due to free carriers and temperature [2], we can

compute the optical modal loss ($\Delta\alpha$) and effective refractive index variation due to FCD or temperature ($\Delta n_{effFC,T}$) as shown in Fig.1 (c).

3 Results

We examine three MMRs with different radius, and different coupling coefficient (k^2) as reported in Table 1 to obtain a Q-factor fixed to $1.3 \cdot 10^5$, using waveguide cross-sections depicted in Fig. 1(a): Si Strip, Si/PolySi Strip and Si/PolySi 3 wings Rib. The silicon rib structure is omitted due to its bend loss exceeding 1 dB/cm.

	Si Strip	Si/PolySi Strip	Si/PolySi 3 wings Rib
R=10 µm	0.3%	0.1%	0.08%
R=60 µm	2%	0.7%	0.5%
R=100 µm	3%	1%	0.7%

Table. 1. The values of coupling coefficient for different radius and waveguide cross-sections.

In Fig 2 (a) and (b), we report an example of our model solutions, namely the spatial distribution of free carriers in the Si/PolySi 3 wings Rib. We observe that the silicon cross-section exhibits a higher free carrier density, leading to increased carrier diffusion compared to the poly-Si structure. The reduced carrier density in poly-Si can be attributed to a higher SRH recombination rate, resulting from a greater number of defects in poly-Si, which also shortens the diffusion length relative to silicon. Considering that Free Carrier Absorption (FCA) is directly proportional to the accumulated carrier density within the waveguide, Fig. 2(c) compares the total number of accumulated carriers across the three different waveguides under identical circulating power P_c. The integrated carriers are determined over an equivalent area, defined as 90% of the optical mode area, by integrating n(x,y) and p(x,y). From this graph, we observe that the Si/PolySi 3 wings Rib has fewer free carriers compared to the other waveguides. This advantage will lead to thermal benefits.

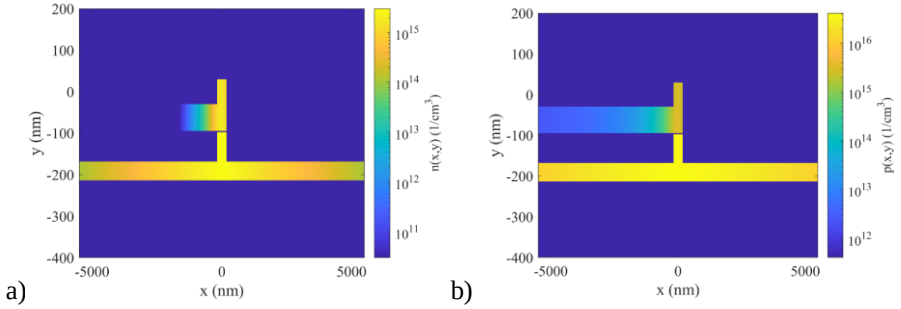

a) b)

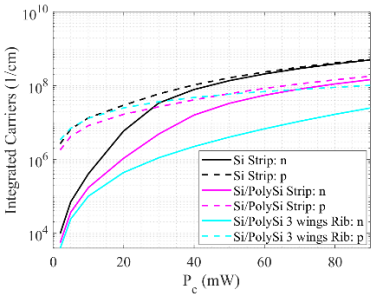

c)

Fig. 2. Example of spatial carriers distribution: (a) electron distribution (n(x, y)) and (b) hole distribution (p(x, y)) in the Si/PolySi 3 wings Rib waveguide due to photon-generation and in for a circulation power equal to 50 mW and radius 10 µm. (c) Integrated total carrier density as a function of the circulating power for each waveguide analysed with radius 10 µm.

The third model solution is the temperature variation of the same example; our observations reveal that the Si/PolySi 3 wings Rib waveguide exhibits reduced heating in comparison to other strip waveguides operating at equivalent circulating powers. This reduced heating is primarily assigned to the presence of lateral wings, which enhance heat dissipation and prevent the concentration of carriers at the center of the waveguide. In Fig. 3 (a), (b) and (c), we present a comparative analysis of the temperature distribution.

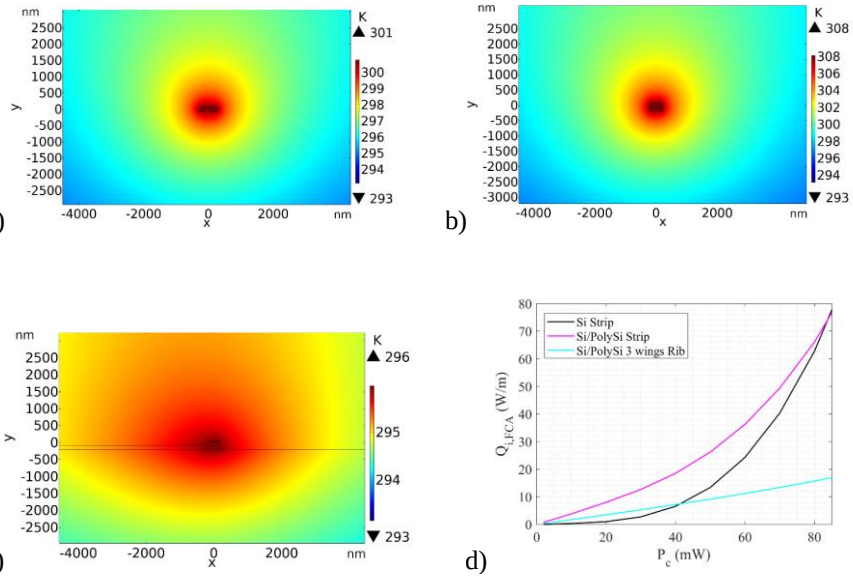

Fig. 3. Example of temperature fluctuation resulting from self-heating for P_c = 50mW and radius 10 µm in (a) Si Strip, (b) Si/PolySi Strip and (c) Si/PolySi 3 wings Rib. (d) Integrated heat source due to FCA over the waveguide cross-section as a function of circulating power with R = 10 µm.

In Fig. 3 (d), we compare the integrated $Q_{i,FCA}$ (heat source due to FCA) across various waveguide cross-sections. For powers below 80mW, the Si/PolySi Strip experiences more heating compared to the Si Strip, which is the result of an higher local modal losses in polysilicon relative to silicon. In additional, the diminished accumulation of carriers in the Si/PolySi 3 wings Rib results in a reduced FCA, consequently minimizing carrier thermalization.

The Si/PolySi 3 wings Rib exhibits lower heat generation compared to others, as such this structure also demonstrates the lowest nonlinear loss for the same circulating power, which is a consequence of the electrons and holes diffusion in the lateral wings of the rib and the faster SRH carrier recombination in poly-Si due to higher trap density [3]. Consequently, this reduces free carrier density where the optical field is confined, leading to smaller modal loss and refractive index variation. The resulting changes in effective refractive index and modal loss are fitted with third-degree polynomials against circulating power, serving as input parameters for calculating the MRR transmission coefficient [4], as shown in Fig.4. In this graph, we can observe that for low bus powers the 3 MRRs have a similar transmission coefficient; but as the power increases, the curve trend changes: for the Si/PolySi 3 wings rib, a smaller NL shift of the resonant wavelength is observed compared to Si Strip and Si/PolySi strip. From the transmission coefficient we can derive the degradation of the quality factor due to nonlinear effects, which varies with the bus power [4]. Consequently, the Si/PolySi 3 wings Rib presents less degradation in transmission coefficient compared to others. In fig. 5 we report for each configuration the maximum input bus power to have a degradation of the Q of less than 10%; the Si/PolySi 3 wings Rib enables reaching a maximum power about 10 dB higher than the standard Si Strip waveguide available in this platform. In Table II, we report the corresponding circulating power and the temperature increase in the core at the maximum input bus power. We observe that for the same waveguide design the circulating power remains almost constant with increasing radius because the increase in bus power is counterbalanced by an increase in radius in all structures. In addition, in the Si/PolySi 3 wings Rib the circulating power is greater than in the other two MRRs and consequently heats up more. However, between the Si/PolySi Strip and the Si/PolySi 3 wings Rib, the circulating power increased 7 times, whereas the temperature increased only 3 times. This difference is attributed to the greater heat dissipation in the latter waveguide design as demonstrated in Fig. 3. (d). We also observed that the temperature variation for the same waveguide structure is constant for the 3 radii because there is a small variation in the circulating power in the three cases.

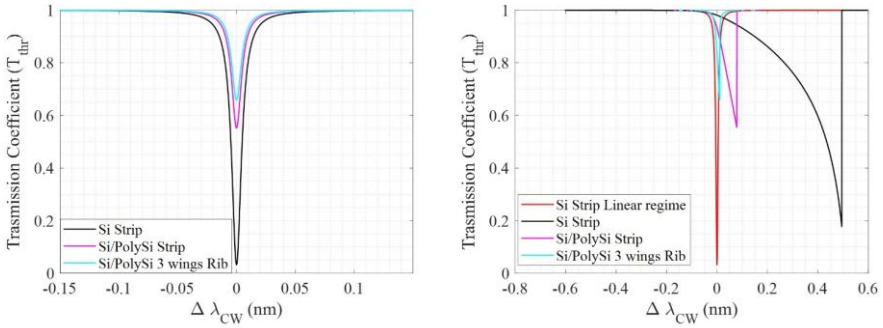

Fig. 4. Example of transmission coefficient of the 3 MRRs as a function of different bus input power: (a) linear regime, (b) P_{bus} = -10 dBm. The radius of MRRs is equal to 10 µm and Q = $1.3 \cdot 10^5$.

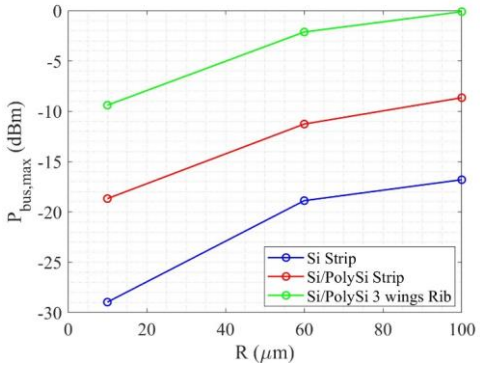

Fig. 5. Maximum bus power, with 10% Q, as a function of radius for each structure analyzed.

	Si Strip	Si/PolySi Strip	Si/PolySi 3 wings Rib
$P_{c,max}$ (mW) @R=10 µm	0.256	0.798	4.6
$P_{c,max}$ (mW) @R=60 µm	0.412	0.725	4.6
$P_{c,max}$ (mW) @R=100 µm	0.423	0.705	4.5
ΔT (K)	0.03	0.15	0.4

Table. 2. Summary of maximum circulating power with a 10% Q-factor dependence on radius for each structure, along with temperature variation in MRRs at resonance where the maximum circulating power is observed ($P_{c,max}$).

4 Conclusions

In summary, our study has implemented a model capable of computing the 2D distribution of free carriers and temperature within the various waveguide cross-sections of MMRs on the SISCAP platform. Through our analysis, we have successfully identified a design solution that effectively mitigates nonlinear effects and self-heating. The Si/PolySi 3 wings Rib waveguide emerges as the most advantageous among the options examined. This structure benefits from the free carrier diffusion in the rib waveguides and heat dissipation, complemented by the addition of the poly-Si waveguide, which diminishes bend loss and reduces free-carrier lifetime through increased SRH recombination within poly-Si traps.

This work is supported by Italian National Recovery and Resilience Plan (NRRP) of NextGenerationEU: partnership on Telecommunications of the Future (PE00000001 – program “RESTART”).

References

1. I. Atoum et al., "Challenges of Software Requirements Quality Assurance and Validation: A Systematic Literature Review," in IEEE Access, vol. 9, pp. 137613-137634, 2021, doi: 10.1109/ACCESS.2021.3117989.
2. W. Zhang et al., "Towards subvolt and half-mm scale silicon MOS-capacitor MZI modulators," 2023 IEEE Silicon Photonics Conference (SiPhotonics), Washington, DC, USA, 2023, pp. 1-2, doi: 10.1109/SiPhotonics55903.2023.10141906.Author, F.: Contribution title. In: 9th International Proceedings on Proceedings, pp. 1–2. Publisher, Location (2010).
3. M. Novarese, S. Romero-Garcia , J. Bovington and M. Gioannini. "Dynamics of Free Carrier Absorption and Refractive Index Dispersion in Si and Si/PolySi Microrings". EEE Photonics Technology Letters, vol. 35, no. 8, pp. 450-453, 15 April, 2023
4. M. Novarese, S. Romero-Garcia, S. Cucco, D. Adams, J. Bovington, M. Gioannini. "Study of nonlinear effects and self-heating in a silicon microring resonator including a Shockley-Read-Hall model for carrier recombination" Vol. 30, No. 9, 25 Apr 2022. Optics Express 14341.